

AN INVESTIGATION ON END MILLING OF ALUMINIUM BASED METAL MATRIX COMPOSITES FOR OPTIMISING MACHINING PARAMETERS

V. Krishnaraj, N. Raghavendran, R. Sudhan and R. Vignesh*

Department of Mechanical Engineering, PSG College of Technology,
Coimbatore, Tamilnadu, India

ABSTRACT

In recent years, the utilization of metal matrix composites (MMC) have increased in engineering fields of automobile, aviation, aerospace, construction and microelectronics. In conjunction with innovations in these advanced materials, machining them to obtain good dimensional accuracy and surface integrity has become a challenge. In this present work, 15 % (by weight) SiC particle reinforced aluminium is synthesized by stir casting technique. The synthesized MMC is end milled using Ø16 mm carbide end mill in a CNC milling machine and the machining parameters explicitly cutting speed, feed rate and depth of cut are optimized for minimum surface roughness and total force acting on the tool using response surface methodology (RSM). The chip formed during the machining process is analyzed using scanning electron microscope (SEM). The un-coated cutting tool insert was compared with the nano-composite coated insert on tool wear at optimised cutting conditions.

Keywords: metal matrix composites (MMC); aluminium; milling; machining parameters

1. INTRODUCTION

Metal Matrix Composites owing to their increased specific strength and stiffness are replacing the conventionally used materials especially in the fields of automobile, aerospace and structural engineering. Due to their low cost, ceramic particles reinforced aluminium alloy are most popular among the MMC. The ceramic particles or reinforcements such as SiC and alumina make machining of composite tougher. This difficulty in machining opens a wide area of research in the processing of these materials.

* Corresponding author: vkr@mec.psgtech.ac.in

Kuan et al. (1999) described that the merchant's circle equation cannot be used for the composite materials as the yield strength of these materials are completely different and also the assumptions made during merchant circle derivation restricts their application to composite materials. They also related the coefficient of chip deformation with the fraction of reinforcement and the shear angle. Ozben et al. (2008) investigated the effects of the reinforcement fraction on the mechanical properties like hardness and tensile strength of the Al/SiC_p composite. Effects of the machining parameters and reinforcement fraction on the tool wear and surface roughness during turning of the Al/SiC_p composite using TiN coated carbide tool were examined by them.

The machinability of Al/SiC_p composite while turning using rhombic tools were reported by Manna et al (2003). BUE and chip formation were examined by them using the SEM micrographs to provide an economic machining solution through their work. Davim et al (2003) reported the influence of the cutting parameters during turning Al/SiC_p on the surface roughness, tool wear and power requirements by employing ANOVA and multiple linear regression techniques. Liu et al. (2002) used PCD turning tools to compare the cutting forces obtained from the conventional turning and ultrasonic vibration turning, there by concluding that the low speed and high depth of cuts reduces cutting forces in ultrasonic vibration turning.

They developed process parameters for turning thin walled Al/SiC_p MMC. Muthukrishnan et al. (2009) turned Al/SiC_p bars using coarse grade PCD inserts under different cutting conditions. The machining conditions were then optimized for minimized surface roughness by employing the ANOVA and ANN. Seeman et al. (2010) developed a mathematical model for machinability evaluation in turning of Al/SiC_p composites. They also described the effects of process parameters on the tool flank wear and surface roughness.

Ge et al. (2008) used PCD tools for ultra precision turning of Al/SiC_p MMC and revealed the effects of the cutting speed and feed rate on the tool workpiece surface integrity. Reddy et al. (2008) end milled Al/SiC_p MMC using TiAlN coated carbide inserts and optimized the cutting parameters for minimized surface roughness using GA. They also found out the micro hardness and residual stress at the optimized cutting conditions. Karakas et al. (2006) studied the effects of the cutting speed on the tool performance in end milling of B₄C_p particles reinforced aluminium MMC.

They also compared the wear performance of the uncoated tool and multi-layer coated tools and found that the triple layer coated tool has better wear resistance. Oktem et al. (2005) applied response surface methodology (RSM) for optimization of machining parameters for minimized surface roughness during milling of the Al-7075 alloy parts. They also used genetic algorithm (GA) for optimizing the parameters for desired surface roughness. Lin et al. (1998) studied the chip formation in turning of the Al/SiC_p MMC using PCD inserts. They analysed the SEM micrographs of the chips formed and found the separation of the matrix and reinforcement within the chip. Joshi et al. (2009) analysed the chip formation mechanism in turning of the Al/SiC_p MMC.

They tried to correlate the quality of the machined surface by analysing the SEM micrographs of the chips formed during turning. Arokiadass et al. (2011) made an attempt to develop a predictive model of surface roughness in end milling of Al/SiC_p MMC. The present work reports the effect of machining parameters on cutting force, surface finish and behaviour of chip during end milling using carbide inserts. Further this paper reports the effect of coating on the tool life in finish milling of metal matrix composites.

2. EXPERIMENTAL PROCEDURE

2.1. Material Synthesizing

The 6061 Al alloy of the following composition (by weight) is chosen as the metal matrix of the composite and the reinforcement is 15% (by weight) SiC powders of size 36 μm . Table 1 and 2 presents the composition of matrix and reinforcement used for the metal matrix composites.

Table 1. Composition of Al-6061 alloy

Al	Mg	Fe	Si	Mn	Others
97.25 %	1.08 %	0.17 %	0.63 %	0.52 %	0.35 %

Table 2. Composition of SiC powders

SiC	SiO ₂	Si	Fe	Al	Free C
99.64 %	0.15 %	0.02 %	0.02 %	0.02 %	0.15 %

The Al/SiC_p MMC with the above composition is synthesized by stir casting process. Figure 1 shows a schematic sketch of the stir casting setup, describing its parts. Table 3 presents the parameters used for synthesising the metal matrix specimen. The micro-hardness of the MMC is found to be as 106 VHN using tested Vickers micro-hardness tester at a load of 100g.

Using optical microscope the microstructure of the synthesized Al/SiC_p MMC is examined. The distribution of the SiC particles and the agglomerations is presented in the Figure 2.



Figure1. Stir casting setup.

Table 3. Experimental Details of Stir casting

Furnace	Induction furnace
Pre – heater	Electric furnace
Mass of Al 6061 alloy	900 g
Mass of SiC reinforcement	135 g
Mass of Mg (wetting agent)	15 g
Melting point of Al 6061	700°C
Pre heat temperature of SiC reinforcement	450 °C
SiC addition temperature	750 °C
Stirrer speed	850 rpm
Time of SiC addition	120 minutes
Post stirring time	20 minutes
Mould preparation	Wooden pattern in green sand

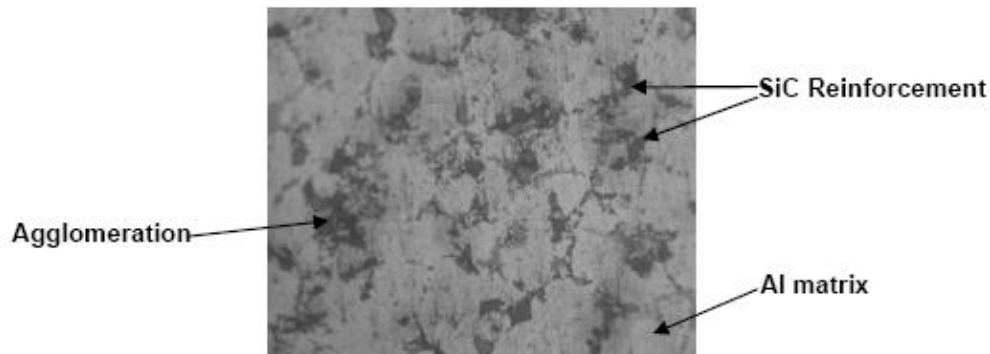


Figure 2. Microstructure of Al/SiCp MMC at 200X.

2.2. Experimental Setup

The end milling experiments are carried out in a 3 axes CNC Makino Vertical Machining Centre Model S33. The experimental setup for end milling is presented in Fig.3. Milling tool dynamometer (SYSCON) is mounted on the milling machine table and the rectangular metal matrix composite specimen is held in its fixture. The dynamometer is interfaced with personal computer (PC) for force measurements. Milling is a very complicated cutting process which involves many parameters such as cutting speed, feed rate, depth of cut and tool geometry, etc. The most influential factors affecting the surface finish and forces acting on the tool were studied by conducting a set of experiments. The factors considered for the experimentation are cutting speed, feed, and depth of cut. The experimental conditions are presented in Table 4. The experiments have been conducted under dry condition in the vertical machining centre.

The tool used for end milling is by an inserted cutter of Ø16 mm made by Sandvik Coromant. The specification of the insert used is R310 11 T3 08E NL-13A. It is an uncoated carbide insert, which is given in Figure 4. One set of insert is coated using nano-composite structured Hyperlox coating by Physical Vapour Deposition (PVD) magnetron sputtering technique. The coating thickness is of 3 µm in order to compare with uncoated insert.

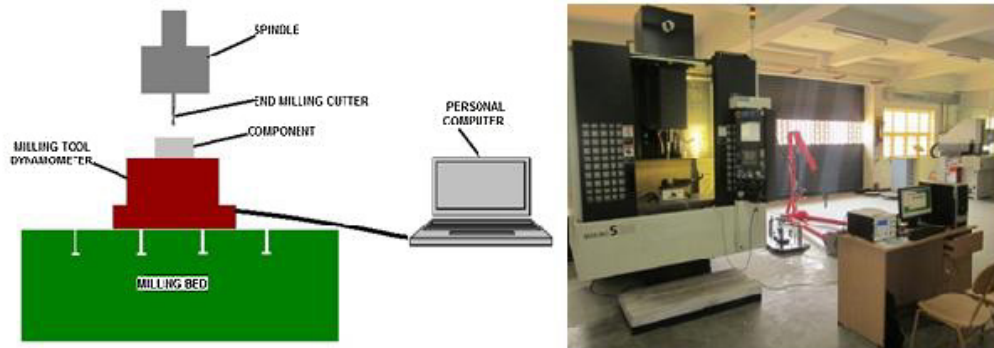


Figure 3. Experimental setup.

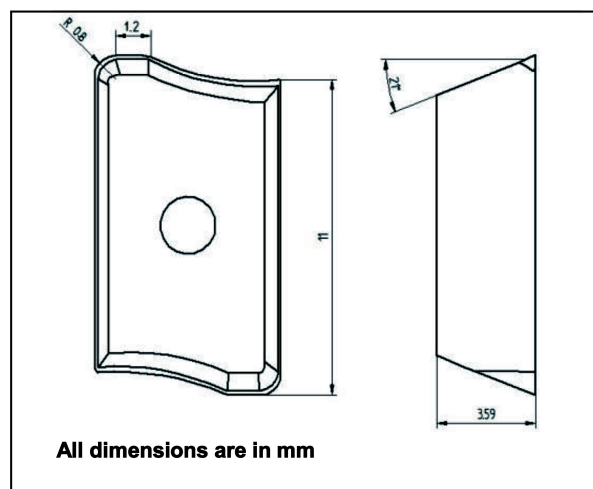


Figure 4. Details of the insert.

Table 4. Machining parameters

Parameter Level	Speed (m/min)	Feed rate (mm/rev)	Depth of cut (mm)
-1	150	0.05	0.10
0	200	0.20	0.15
1	250	0.35	0.20

Using central composite design (CCD), totally 16 experiments are carried out. For each run, the forces acting on the tool are measured using tool dynamometer. The surface roughness is measured by Taylor Hobson surface roughness tester with a cut-off length of 2.5 mm. The surface roughness is measured at 3 different places in a machined surface and average of these values is taken. The machining parameters are optimized using RSM. For the optimized machining condition, the effect of Hyperlox coated inserts on the surface roughness and tool wear are analysed by comparing the results of the experiments conducted using coated and uncoated inserts under dry condition.

3. RESULTS AND DISCUSSION

Milling can generally be classified as rough milling and finish milling. In case of rough milling the major factor to be considered is the material removal rate whereas in finish milling it is surface roughness. In both the cases the tool life is expected to be longer. The improvement in surface finish and tool life can be accomplished by optimizing the machining conditions or by changing the tool conditions. Here under both the conditions experiments are conducted, the results are discussed below.

3.1. Response Surface Regression Analysis

Response surface model (RSM), which is an analytical function, in predicting surface roughness and tool force values is developed using RSM. RSM uses statistical design of experiment (experimental design) technique and least-square fitting method in model generation phase.

The initial stage in creating a RS model is to design experiments using one of the RSM designs. Here, Central Composite Design (CCD) is used for experimental design. A face-centred experimental design with 3 factors (speed, feed rate, depth of cut) and 20 runs is generated using CCD in the MINITAB software.

Among the 20 runs, 4 centre point runs are ignored and totally 16 runs of experiments are conducted. The tool forces are measured using Syscon Milling tool dynamometer. The forces acting on the tool are shown in the Figure 5. The tangential and feed forces are considered vital over the thrust force. The total force acting on the tool is then calculated as the vector sum of the tangential and feed force.

The surface roughness (R_a) is measured using Taylor Hobson surface roughness tester (shown in Figure 6) with a cut-off length of 2.5 mm. At each slot, the surface roughness is calculated at 3 different spots and their average is taken as the average surface roughness. Table 5 shows the list of experiments conducted and the tool force and surface roughness obtained at each run.

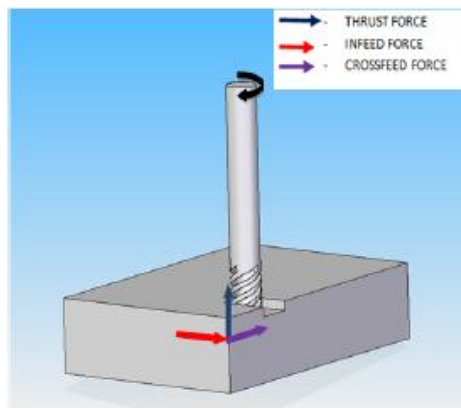


Figure 5 Forces acting on the tool.

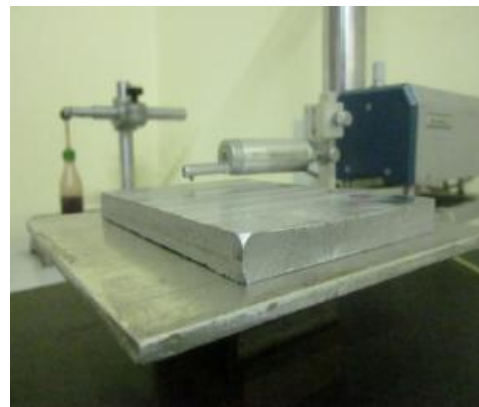


Figure 6. Surface roughness tester.

Table 5. Experimental results of milling

T. No.	C.Speed, V (m/min)	Feed rate, f (mm/rev)	Depth of cut, d (mm)	Total force, F (N)	Surface roughness, R _a (μm)
1	150	0.35	0.10	27.74	1.58
2	150	0.05	0.10	31.02	2.28
3	150	0.05	0.20	13.87	1.33
4	250	0.05	0.20	21.93	1.44
5	200	0.35	0.15	71.41	2.82
6	200	0.20	0.15	59.67	2.25
7	250	0.05	0.10	57.20	1.06
8	250	0.35	0.10	130.88	1.65
9	200	0.20	0.10	136.63	2.04
10	150	0.20	0.15	39.24	2.62
11	200	0.05	0.15	19.62	2.30
12	150	0.35	0.20	49.05	2.65
13	200	0.20	0.15	59.67	2.65
14	250	0.20	0.15	74.71	2.38
15	200	0.20	0.20	69.36	2.34
16	250	0.35	0.20	69.36	2.42

The obtained results are analysed using the MINITAB software. The speed, feed rate and depth of cut are chosen as the independent variables or the factors and the surface roughness and tool force are chosen as the dependent variables or responses.

Response surface regression equation for cutting force (F) is given in Eq. 1

$$\begin{aligned}
 F = & -150.253 + 3.662V + 325.23f - 2762.29d - 0.00704V^2 \\
 & - 1291.42f^2 + 11370.6d^2 + 1.486Vf - 5.046Vd \\
 & + 203.382fd
 \end{aligned}$$

(R² = 0.908) (1)

Response surface regression equation for surface roughness (R_a) is given in Eq.2

$$\begin{aligned}
 R_a = & -1.668 + 0.0144V - 5.303f + 43.254d - 0.00007V^2 \\
 & - 5.20307f^2 - 194.828d^2 + 0.0158333Vf + 0.0515Vd \\
 & + 40.1667fd
 \end{aligned}$$

(R² = 0.8895) (2)

3.2. RS model Analysis

The developed mathematical models are subjected to ANOVA and F ratio test to justify their goodness of fit. The calculated values of F ratios for lack-of-fit are compared to standard values of F ratios corresponding to their degrees of freedom to find the adequacy of the

developed mathematical models. The F ratio is calculated from ratio of mean sum of square of source to mean sum of experimental error.

The standard percentage point of F distribution for 95 % confidence level is 4.06 (Seeman et al., 2010). The results of analysis in the Tables 6 and 7 reveal that the actual F values 1.19 and 1.05 which are less compared to the standard F value and thus adequate within the 95% confidence limit.

Table 6. Analysis of Total force RS model

Source	Degrees of freedom	Sum of squares	Adjusted Mean of squares	F value	P value
Regression	9	17275.5	1919.50	6.62	0.016
Linear	3	10482.7	836.69	2.89	0.125
Square	3	4505.9	1501.98	5.18	0.042
Interaction	3	2286.9	762.30	2.63	0.145
Residual error	6	1739.2	289.86	-	-
Lack of fit	5	1489.6	297.91	1.19	0.589
Pure error	1	249.6	249.64	-	-
Total	15	19014.7	-	-	-

Table 7. Analysis of Surface roughness RS model

Source	Degrees of freedom	Sum of squares	Adjusted Mean of squares	F value	P value
Regression	9	3.81293	0.42366	5.10	0.030
Linear	3	1.20891	0.13437	1.62	0.281
Square	3	1.63259	0.54420	6.56	0.025
Interaction	3	0.97144	0.32381	3.90	0.073
Residual error	6	0.49801	0.08300	-	-
Lack of fit	5	0.41801	0.08360	1.05	0.627
Pure error	1	0.08000	0.08000	-	-
Total	15	4.31094	-	-	-

The contribution of the cutting parameters on the dependent Variables (DV) namely surface roughness and tool force can be studied by Pareto chart which gives the significance of each term in the generated RS model in terms of standardized effect estimate. Using STATISTICA 10.0, the Pareto chart is obtained for the total force and surface roughness RS models as shown in figures 7 and 8 respectively.

In the Pareto chart, L denotes that the term is linear, Q denotes that the term is quadratic. Also 1, 2 and 3 stands for speed, feed and depth of cut respectively. From Figure 7 it is understood that the total force is highly influenced by feed rate and speed. This may be due to the fact that the tangential force component opposes the rotational movement of the tool at cutting edges and the feed force is the one that directly opposes the feed motion of the tool. A keen observation of Table 5 will reveal the fact that the force changes highly with respect to feed rate compared to other two parameters.

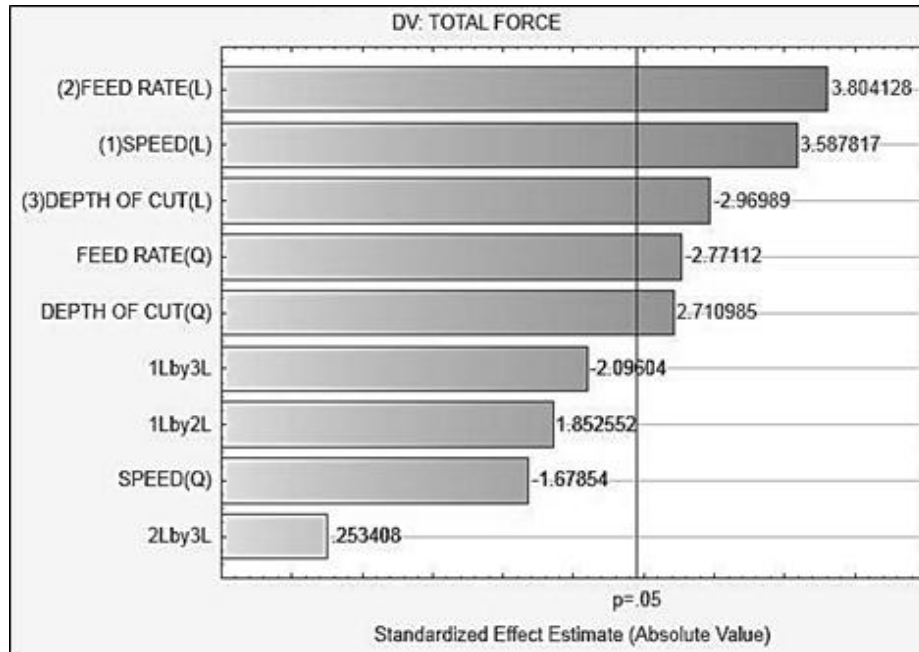


Figure 7. Pareto chart for Total force RS model.

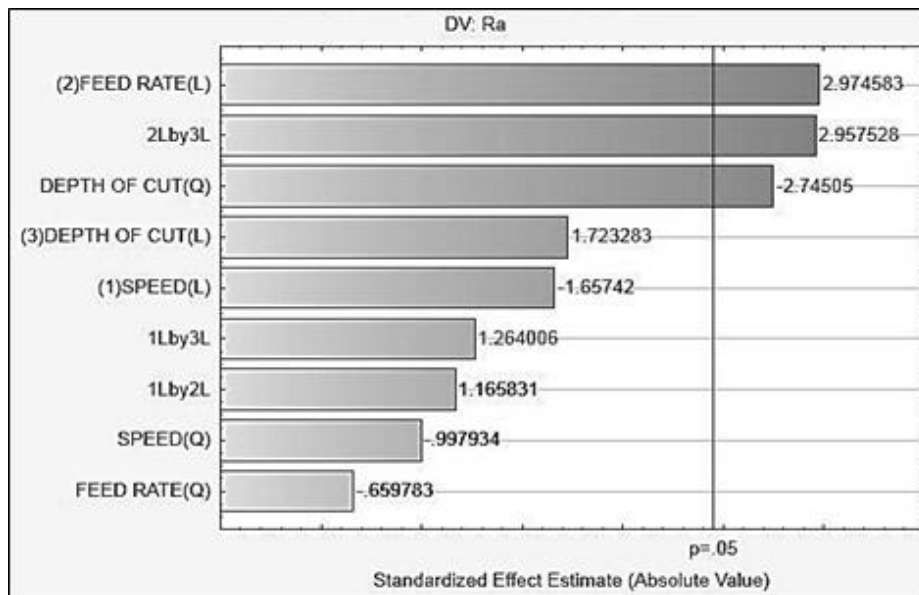


Figure 8. Pareto chart for Surface roughness RS model.

From Figure 8 it is clearly understood that the surface roughness is highly influenced by feed rate and the interacted feed rate and depth of cut. Also from the Table 5 it can be observed that the surface roughness decreases with increased cutting speed which is a usual trend (Suresh Kumar et al., 2008). This can be due to the reason that at high cutting speed the heat flow time shortens resulting in the softening of the material and thereby aiding in grain boundary dislocation thus reducing the surface roughness. Whereas the feed rate reduction

reduces the cut chip thickness resulting in the lesser cutting forces and improved surface finish. The increase in depth of cut leads to increased abrasive contact area between tool and material thereby causing sufficient heat generation to produce Built-up Edges (BuE) resulting in reduced surface finish (Davim 2011). The interaction effects on the dependent variables (DV) can be studied using surface and contour plots. Surface plots explain the effects effectively than the contour plots. The surface plot for the total force and surface roughness are shown as below. In plotting the above surface plots, a constant value is applied for third independent variable. In Figure 9(a) depth of cut is maintained as 0.15 mm, and in Figure 9(b) and Figure 9(c) feed rate is 0.2mm/rev and cutting speed 200 m/min respectively. So, by fixing one of the independent variables, the other two independent variables can be varied for the required output using surface plots. This method can be utilised for machining at low tool forces and increased surface finish. Similar graphs (Figure 10.a-c) were obtained for the effect of machining parameters on surface roughness (Ra)

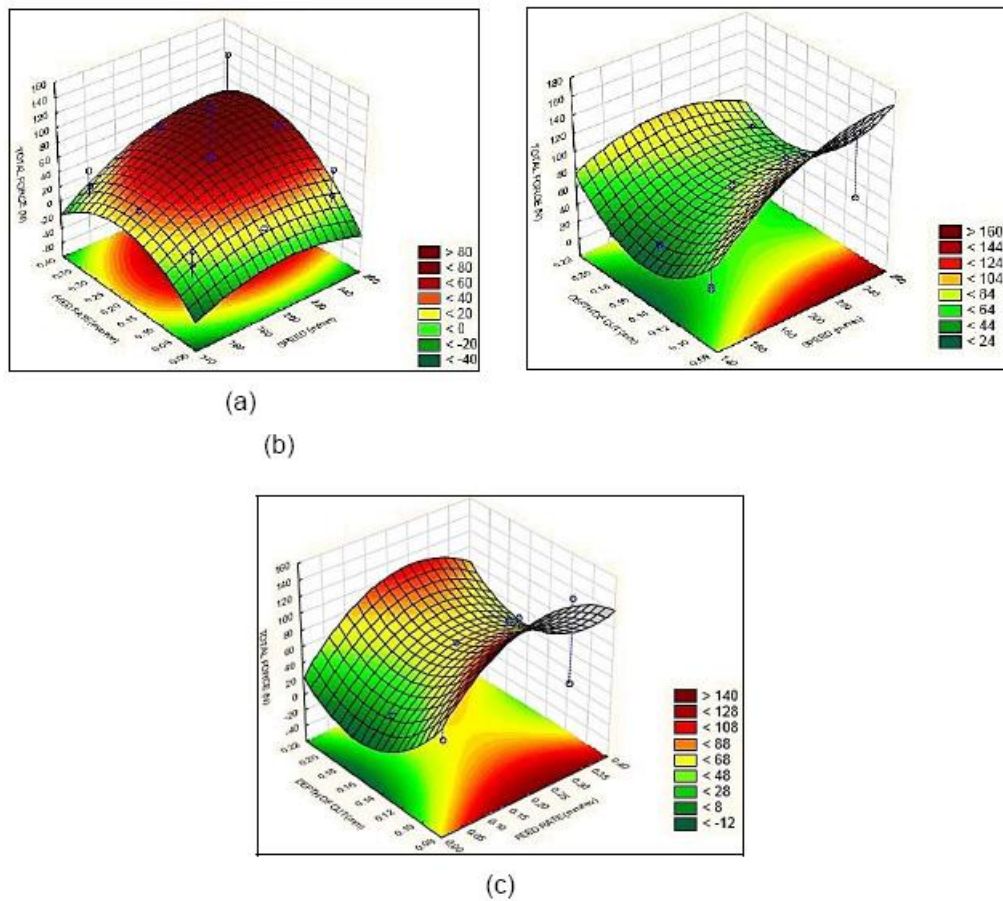


Figure 9. (a) Feed rate, Speed (Vs) Total force (b) Depth of cut, Speed (Vs) Total force. (c)Depth of cut, Feed rate (Vs) Total force.

Apart from the above analysis optimized values for machining parameters are obtained for minimum tool force and minimum surface roughness using the response surface optimizer. Those values are given in the Table 8.

Table 8. Response Surface Optimizer result

Speed (m/min)	Feed rate (mm/rev)	Depth of cut (mm)	Tool force (N)	Surface roughness (μm)
250	0.05	0.20	8.9291	1.2639

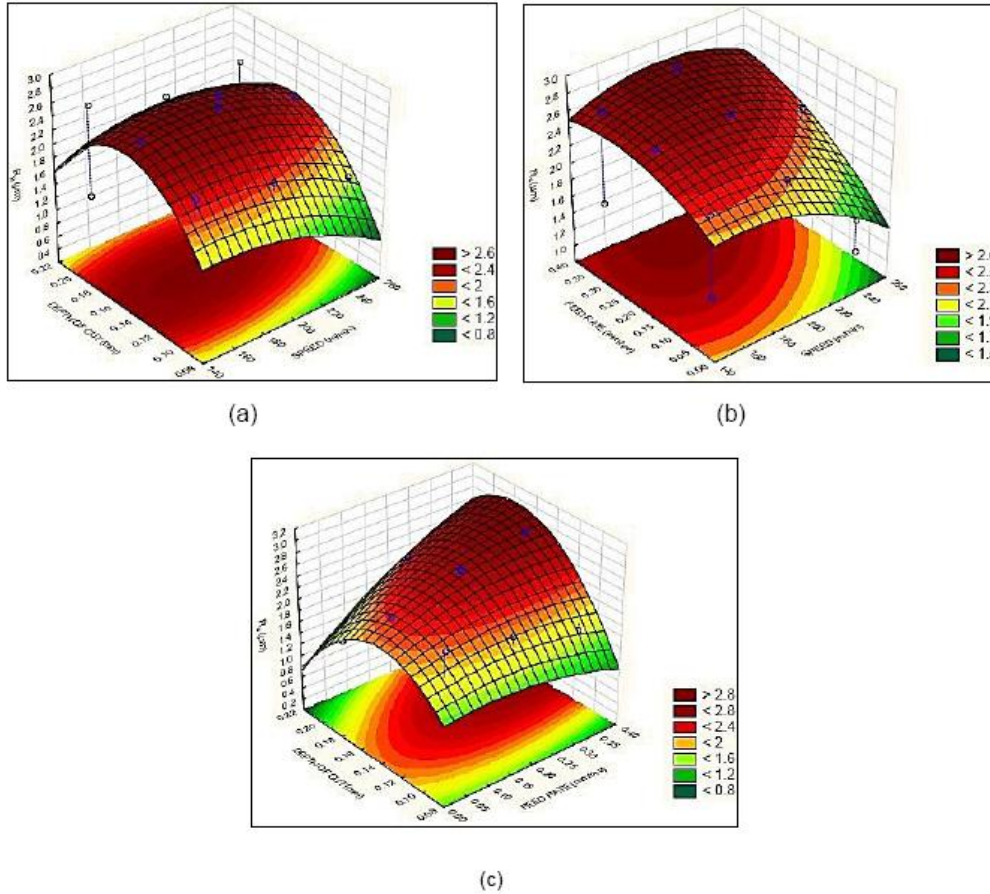


Figure 10. (a) Speed, Depth of cut (Vs) R_a (b) Feed rate, Speed (Vs) R_a (c) Depth of cut, Feed rate (Vs) R_a .

The optimized value has a composite desirability of 0.93 which shows that the multiple-objective optimization is highly reliable. The optimization algorithm used here is “Minimum the Best”.

4. PREDICTION OF OUTPUT USING ANN

A neural network is a network of many simple processors (units) each having a small amount of local memory operating in parallel. The units are connected by communication channels (connections), which usually carry numeric data, encoded by one of the various

ways. One of the best-known examples of a biological neural network is the human brain. The Artificial Neural Network is developed to try to emulate this biological network for the purpose of learning the solution to a physical problem from a given set of examples. The general architecture of a 3-layered Multi-layer Perceptron (MLP) is shown in Figure 11.

MLP uses back propagation algorithm (BPA) for training the network in a supervised manner. This learning process has two operations or passes namely forward and backward pass.

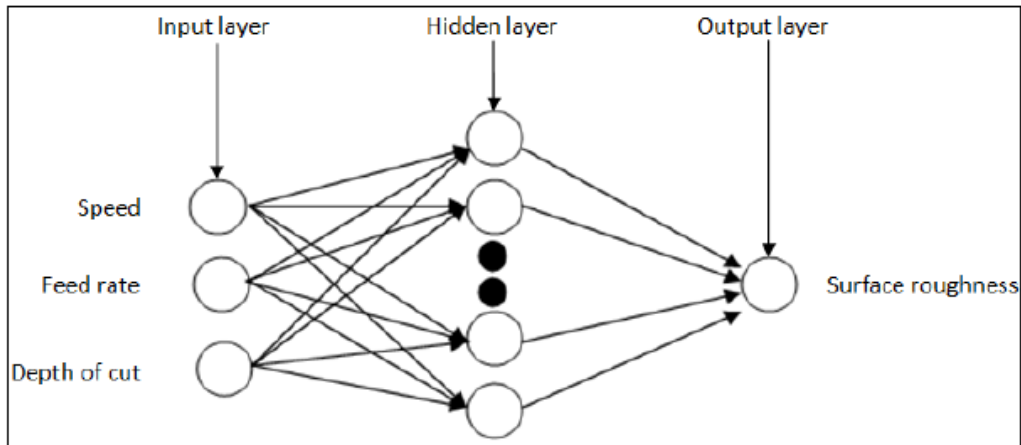


Figure 11. Architecture of Neural network.

During forward pass, data is read and the weights are fixed at input nodes. During backward pass, the error between the desired and the predicted output updates the weights accordingly. In this way, weight values are adjusted in an iterative fashion while moving along the error surface to arrive at minimal range of error, when input patterns are presented to the network for learning the network (Muthukrishnan and Paulo Davim, 2009).

ANN for the current problem is generated using Neural Network tool (GUI) in MATLAB R2010a. The typical observations of the output response comprises of the parameters as shown in Table 12. The network performance is defined by these observations.

Table 12. Typical observations of network performance

PARAMETER	DESCRIPTION/ VALUE
Network configuration	3 – 40 – 1
Number of hidden layer	1
Number of hidden neurons	40
Transfer function used	Logsig(sigmoid)
Number of patterns used for training	12
Number of patterns used for testing	2
R value	0.9536
Number of epochs	1000
Learning factor (η)	0.7
Average Error	0.56 %

The surface roughness results predicted using the generated neural network is shown in the Table.13. Comparing these results with the experimental values and values obtained using RS model yields the error in the prediction process.

By using 40 neurons the average error in ANN prediction of surface roughness is reduced to 0.56 %, whereas the average error in RS prediction is 8.55%. This clearly depicts that ANN offers more accuracy over RS prediction of surface roughness. The maximum error percentage in each case is highlighted in the Table 13. A bar chart showing the variation in the predicted and actual values is plotted in Figure 12.

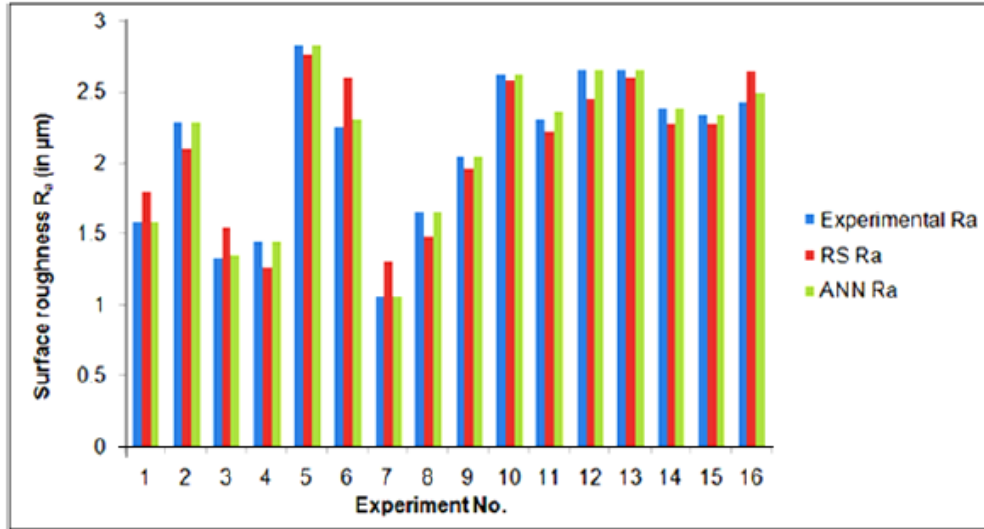


Figure 12. Comparison of ANN and RS prediction.

Table 13. Comparison of ANN, RS and Experimental results

Trial No.	Experimental R_a	ANN prediction of R_a	RS prediction of R_a	% error in ANNPrediction	% error in RS Prediction
1	1.58	1.580127	1.794	0.008	13.54
2	2.28	2.279932	2.092	0.003	8.24
3	1.33	1.349071	1.546	1.434	16.24
4	1.44	1.439931	1.264	0.004	12.22
5	2.82	2.820303	2.755	0.010	2.30
6	2.25	2.300046	2.601	2.224	15.60
7	1.06	1.060023	1.295	0.002	22.19
8	1.65	1.649795	1.472	0.012	10.78
9	2.04	2.039954	1.957	0.002	4.06
10	2.62	2.620057	2.575	0.002	1.71
11	2.30	2.352788	2.213	2.295	3.78
12	2.65	2.650007	2.453	0.0002	7.43
13	2.65	2.650046	2.601	0.001	1.85
14	2.38	2.380136	2.273	0.005	4.49
15	2.34	2.340046	2.271	0.002	2.94
16	2.42	2.490259	2.646	2.903	9.34

5. CHIP FORMATION MECHANISMS

Chips can generally be classified as continuous, discontinuous, and continuous with BuE and serrated chips. Due to the presence of abrasive particles in the MMC, the chips formed are discontinuous most of the time. But at higher feed rates, saw toothed chips with primary cracks at the outer free surface and secondary cracks at the inner surface with BuE were observed. A few SEM micrographs will aid in visual compliance of the above. The SEM micrograph in Figure 13 shows the top surface of a chip. Cracks are predominantly formed because the 15% of SiC particle reinforcement has induced high brittleness in the material by reducing its ductility. This results in formation of discontinuous chips.

The chip formation mechanism can be now revealed as initiation of crack from outer free surface due to shear stress induced by tool rake. And during machining at shear zones, the separation of particle and matrix results in voids caused by the stress concentration at the edge of particles (Lin et al., 1998). These stress components along with the help of voids results in crack propagation and discontinuous chip formation. The saw tooth profile is formed due to highly strained inner surface where the reinforcement is coarsely distributed (Uday et al, 2009) see Figure 13.

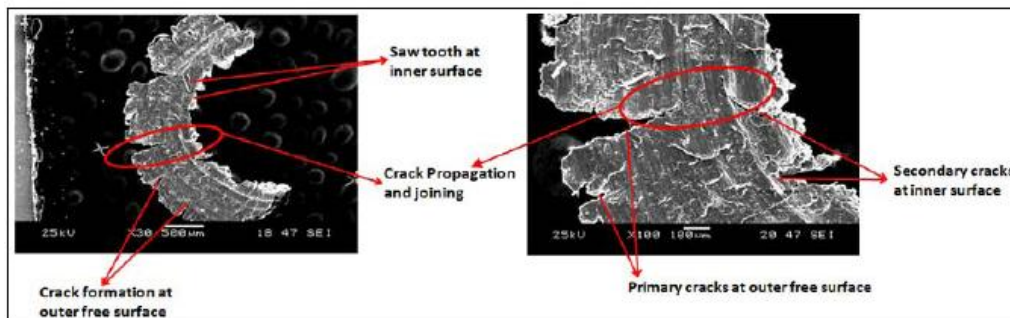


Figure 13. Micrograph of chips showing crack formation.

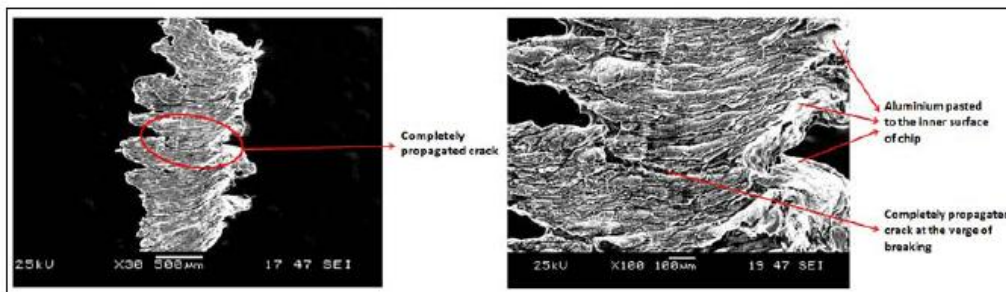


Figure 14. Micrograph of chips showing completely propagated crack.

Figure 14 shows the views of sheared (bottom) surface of a chip. It shows a completely propagated chip which is about to break. We can also see that aluminium is pasted to the edges of the chip. This localized melting of aluminium occurs at the shear zones where the reinforcement concentration is high at the time of material removal. Owing to the low heat

conductivity of SiC particles, aluminium absorbs most of the heat from the shear zone and gets melted.

6. EFFECT OF HYPERLOX COATING ON TOOL WEAR

Optimization is generally done in machining of MMC due to the fact that compared with other materials, tool wear soars while machining them. Reasons behind are the mechanical and thermal loads acting on the tool (Teti R, 2002). Mechanical loads are abrasion caused by contact with the reinforcement particles, alternating stress due to inhomogeneity of the material and dynamic loads caused by the reinforcement impacts at the cutting edge. Contributing to the thermal loads are relatively low cutting temperature (limited by the melting point of the Aluminium matrix material when compared with the SiC reinforcement) and high local temperature generated by intensive micro-contact between cutting edge and reinforcement. Uncoated carbide inserts when subjected to machining undergoes massive wear at their cutting edges. This worn out inserts result in reduced material removal rate and poor dimensional accuracy. This problem can be solved by using coated inserts and PCD inserts. Even though PCD inserts perform well, due to their high cost, coated inserts are preferred. Some of the generally used insert coatings are TiAlN, diamond like carbon (DLC), Hyperlox, Tinalox and diamond coatings. Coatings provide high flank wear resistance which is the common wear that takes place in all metal cutting operations. In case of MMC, the reinforcement wears out the cutting edge by abrasion. This wear mechanism hinders the use of TiAlN coating for MMC as they have less abrasion resistance. Hyperlox coating comprises of a nano-composite structured 2nd generation AlTiN supernitride and it results in a 32% increase in tool life when compared with TiAlN coating (Davim, 2011). The general properties of the coating applied in our case are shown in Table 14.

Table 14. Properties of Hyperlox

S. No.	Properties	Description
1.	Composition	2 nd Generation AlTiNsupernitride
2.	Coating Structure	Nanocomposite
3.	Colour	Black Anthracite
4.	Micro Hardness	3700 VHN
5.	Maximum Application Temperature	1100 ° C
6.	Coating thickness	3 µm at the nose of insert



Figure 15. Insert before and after coating.

Table 15. Experimental results under optimized machining conditions

Machining time (s)	Peak flank wear, VB_{max} (μm)	
	Uncoated inserts	Coated inserts
17	43	27
34	89	62
51	136	99
68	166	130
86	197	155
103	253	182
150	-	248

At the optimized cutting conditions, experiments are conducted until flank wear reaches 0.25 mm with uncoated inserts and coated inserts separately. The peak flank wear VB_{max} is measured after each run using Digital Tool Maker's microscope. The results of the experiment are listed in Table 15.

The flank wear obtained from the experiments are plotted against the machining time in Figure 16. It is revealed from the Figure 17 that the life of the uncoated insert for 0.25 mm wear is 103s whereas it is 150s for coated insert. Hereby, we can observe that the Hyperlox coating results in a 45.6% increase in tool life.

AlTiN coatings with their higher Al content can offer better thermal resistance than TiAlN coatings. Silicon content in the coating which surrounds AlTiN crystallites as a silicon nitride binder ensures that a fine nanostructure is maintained up to 1200°C, therefore, the hardness loss at high temperature is minimized. This ensures that coating has sufficient hardness to resist abrasion of the reinforcement. Thus, wear caused by both thermal and mechanical loads are reduced by Hyperlox coating.

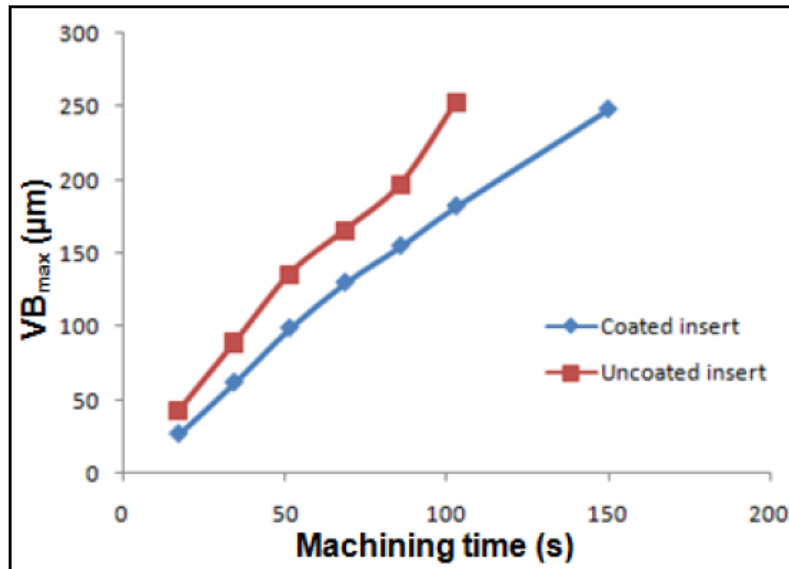


Figure 16. Machining time (Vs) Flank wear.

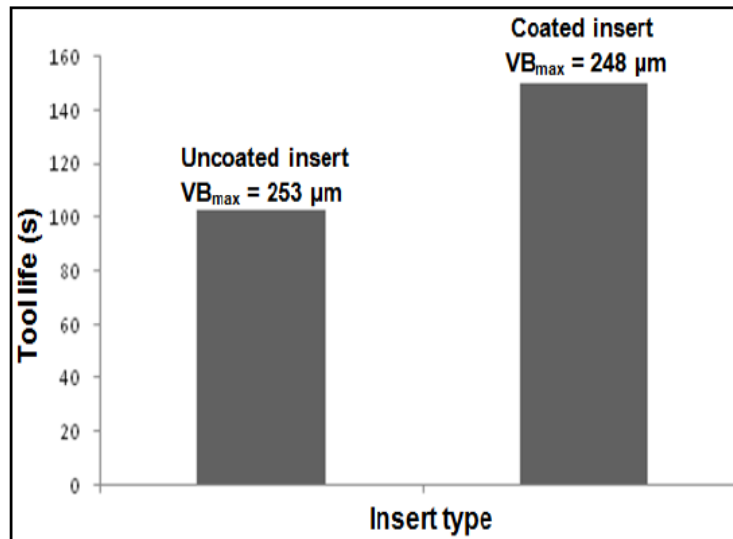


Figure 17. Tool life comparison chart.

CONCLUSION

The following conclusions could be drawn from the experimental analysis.

1. The tool force is found to be highly affected by the cutting speed followed by feed rate when compared to depth of cut.
2. The surface finish obtained is better at high speeds and low feed rates. Also depth of cut is found to have a negative effect on the surface finish.
3. The optimized parameters obtained are 247.83 m/min, 0.05 mm/rev and 0.19 mm for a tool force and surface roughness of 8.74 N and 1.26 μm respectively.
4. The neural network developed for estimating surface roughness is found to be accurate than response surface method.
5. The chips formed are generally discontinuous and at high feed rates it contains BuE and Saw tooth at their inner surface.
6. The tool life is increased by 45.6 % with help of Hyperlox coating and the Al sticking is found to be marginally higher in coated inserts which could be because, the Hyperlox coating is highly heat resistant coating. This high heat resistance of the Hyperlox coating melts the Al in the MMC rapidly than the uncoated inserts. Also this can be accounted due to the presence of Al in the Hyperlox coating.

REFERENCES

- Arokiadass R, Palaniradja K, Alagumoorthi N(2011), "Predictive modeling of surface roughness in end milling of Al/SiCp metal matrix composite", *Archives of Applied Science Research*,3 (228 – 236).

- Ge Y F, Xu J H, Yang H, Luo S B, Fu Y C (2008), "Workpiece surface quality when ultra-precision turning of SiCp/Al composites", *Journals of Materials Processing Technology*, 203 (166 – 175).
- Lin J T, Bhattacharyya D, Ferguson W G (1998), "Chip Formation in the machining of SiC – Particle Reinforced Aluminium – Matrix Composites", *Composites Science and Technology*, 58 (285 – 291).
- Liu C S, Zhao B, Gao G F and Jiao F (2002), "Research on the characteristics of the cutting force in the vibration cutting of a particle reinforced metal matrix composites SiCp/Al", 129(1-3), (196 – 199).
- Manna A and Bhattacharyya B (2003), "A study on machinability of Al /SiC – MMC", *Journals of Materials Processing Technology*, 140 (711- 716).
- Miracle D B (2005), "Metal Matrix Composites – from science to technological significance", *Composites Science and Technology*, 65 (2526 – 2540).
- Muthukrishnan N and Paulo Davim J (2009), "Optimization of machining parameters of Al/SiC-MMC with ANOVA and ANN analysis", *Journals of Materials Processing Technology*, 209 (225 – 232).
- Oktema H, Erzurumlu T, Kurtaran H (2005), "Application of response surface methodology in the optimization of cutting conditions for surface roughness", *Journals of Materials Processing Technology*, 170 (11 – 16).
- Paulo Davim J (2003), "Design of optimisation of cutting parameters for turning metal matrix composites based on the orthogonal arrays", *Journals of Materials Processing Technology*, 132 (340 – 344).
- Paulo Davim J (Ed) (2011), "*Machining of hard metals*", Springer.
- Quan Y M, Zhou Z H, Ye B Y (1999), "Cutting process and chip appearance of aluminium matrix composites reinforced by SiC particle", *Journals of Materials Processing Technology*, 91 (231-235).
- Seeman M, Ganesan G, Karthikeyan R, Velayudham A (2010), "Study on tool wear and surface roughness in machining of particulate aluminum metal matrix composite-response surface methodology approach", *Journal of Advanced Manufacturing Technology*, 48 (613 – 624).
- Serdar Karakas M, Adem Acir, Mustafa Ubeyli, Bilgehan Ogel (2006), "Effect of cutting speed on tool performance in milling of B4Cp reinforced aluminum metal matrix composites", *Journals of Materials Processing Technology*, 178 (241–246).
- Suresh Kumar Reddy N, Shin Kwang-Sup, Minyang Yang (2008), "Experimental study of surface integrity during end milling of Al/SiC particulate metal–matrix composites", *Journals of Materials Processing Technology*, 201 (574 – 579).
- Tamer Ozben, Erol Kilickap and Orhan Cakir (2008), "Investigation of mechanical and machinability properties of SiC particle reinforced Al-MMC", *Journals of Materials Processing Technology*, 198 (220 – 225).
- Teti R (2002), "Machining of Composite Materials", *CIRP Annals– Manufacturing Technology*, 51(2) (611 - 634).
- Uday A. Dabade, Suhas S. Joshi (2009), "Analysis of chip formation mechanism in machining of Al/SiCp metal matrix composites", *Journal of Materials Processing Technology*, 209, (4704 – 4710).

Reproduced with permission of the copyright owner. Further reproduction prohibited without permission.